JOURNAL OF MATERIALS SCIENCE 12 (1977) 117–125

Sub-critical crack extension and crack resistance in polycrystalline alumina

H. HÜBNER, W. JILLEK
Institut für Werkstoffwissenschaften (Materials Science), University Erlangen-Nürnberg, D-852 Erlangen, Martensstraße 5, Germany

Sub-critical crack extension can readily be observed in controlled fracture tests in four-point bending. A natural crack of any desired length c which exceeds the notch depth c_0 by the amount $\Delta c = c - c_0$ can be introduced into bend specimens by stable crack propagation. The stress intensity factor to achieve Δc increases considerably with increasing Δc. In pre-cracked specimens the stress intensity factor K_{I0} to start the crack and the critical value K_{IC} strongly depend on the natural crack length Δc whereas K_{I0} and K_{IC} are independent of c_0 in solely notched specimens. From a quasi-continuous evaluation of the load–deflection curve recorded during controlled fracture, the "differential work of fracture" can be obtained as a function of the achieved crack length. It may be regarded as the crack extension resistance R of the material because the balance between the energy release rate $\mathcal{G}_I$ and R is maintained throughout the experiment. By that, a formal analogy to the R-curve concept of fracture mechanics is given. The steady increase of R is explained by multiple crack formation and by the interference of the fracture surfaces due to the angular development of the crack front.

1. Introduction

The extension of cracks in ceramic materials at values of the stress intensity factor K_I well below the critical level K_{IC} has been reported by many authors. A survey of the literature on the subject of sub-critical crack growth has been given recently by Wiederhorn [1]. The process of crack propagation can be described by the K, v-relationship of polycrystalline alumina at room temperature [2], and Wiederhorn *et al.* [3] reported crack velocity measurements on sapphire at various temperatures in vacuum.

Sub-critical crack growth is the reason for the phenomenon of delayed failure of most ceramic materials. Davidge *et al.* [4], Evans [5], and Evans and Wiederhorn [6] have shown the connection between the sub-critical extension of inherent flaws and the time-to-failure in a ceramic material. Once the dependence of v on K_I is known, the time-to-failure of a sample under constant or varying stress can be predicted and vice versa [1, 5, 6]. Thereby the strength–probability–time diagram of the material may be established [4].

Sub-critical crack growth in brittle materials is attributed to a thermally activated process which is assisted by the applied stress. Several mechanisms have been proposed:

(1) the breaking of thermally fluctuating lattice bonds [7];

(2) the diffusion of vacancies in the stress gradient to the crack tip [8];

(3) the formation and motion of kinks along the crack front [9].

The activation barrier for cracking can be reduced considerably by the attack of a corrosive environment. In the case of alumina, the rate of the process is accelerated in the presence of water vapour by several orders of magnitude [2].

Sub-critical crack growth can readily be observed in controlled fracture tests. In many experiments performed by the authors to determine the work of fracture using Nakayama's method of stable crack propagation [10], a pronounced deviation of the load–deflection curve from the elastic behaviour has been found. Fig. 1 shows

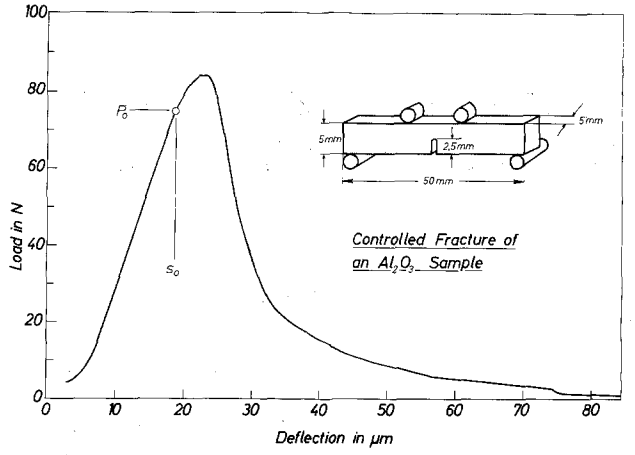

Figure 1 Load–deflection record of a controlled fracture test. The deviation from the elastic increase is indicated by P_0 and s_0.

a record of a completely stable experiment. Before the maximum load is reached, the curve bends at load P_0 and deflection s_0 indicating the beginning of crack extension from the root of the machined notch at a stress intensity factor K_{I0}.

This paper describes investigations on the formation and extension of sub-critical cracks at deflections $s > s_0$ (Fig. 1) and the quantitative determination of the resulting crack length Δc. The dependence of the crack length Δc on the applied stress intensity factor K_I is established. The influence of cracks formed sub-critically by repeated loading and unloading on K_{I0} and K_{IC} is reported. The results are interpreted in terms of the "crack resistance" of the material analogous to the treatment of the crack behaviour of metallic materials.

2. Experimental technique

Commercially available pure alumina (Degussit AL 23) was used throughout the experiments (MgO content 0.5%, porosity 4%, average grain size 18 µm). Specimens were cut from plates and ground in the form of bars of about 4 mm × 5 mm × 50 mm. The bars were centre notched with a diamond cutting blade of 0.10 mm width producing a notch width of 0.13 mm. The notch depth c_0 varied between 20 and 40% of the sample width.

Controlled fracture experiments were carried out in a universal testing machine (Instron Corp.) using a 5000 N load cell and a cross-head speed of 5 µm min^{-1}. The specimens were loaded in four-point bending. The upper span was 10 mm and the lower span varied between 45 and 48 mm (see Fig. 1). The load was recorded against the deflection of the specimen. The elastic deformation of the rollers, of the loading plates, and of all other parts of the bending system which contribute to the measured deflection were determined separately and subtracted from the total deflection to obtain the true specimen compliance.

3. Sub-critical crack extension

3.1. Determination of crack length from the specimen compliance

The extension of cracks in the region $P > P_0$ where the load–deflection curve deviates from the elastic behaviour was determined from a compliance measurement in a subsequent bend test. The determination of the crack length from the specimen compliance is sometimes used in opaque materials when an optical measurement is difficult or impossible. An application to double torsion specimens has been reported by McKinney and Smith [11]. A precise experimental method for measuring the compliance of single edge notch bend specimens has been described [12]. This method was used in the present work.

After Irwin [13] the relationship

$$\mathcal{G}_I = (P^2/2bh)\, d\lambda/dX \qquad (1)$$

exists between the energy release rate $\mathcal{G}_I$, the load P, and the specimen compliance λ (b and h are the thickness and the width of the specimen respectively, and c is the crack length, $X = c/h$ is the relative crack length). The stress intensity factor K_I is

$$K_I = \sigma\sqrt{c}Y \qquad (2)$$

where the applied stress σ is proportional to P. By inserting Equations 1 and 2 into Irwin's equation [13]

$$K_I^2 = \mathcal{G}_I \cdot E', \qquad (3)$$

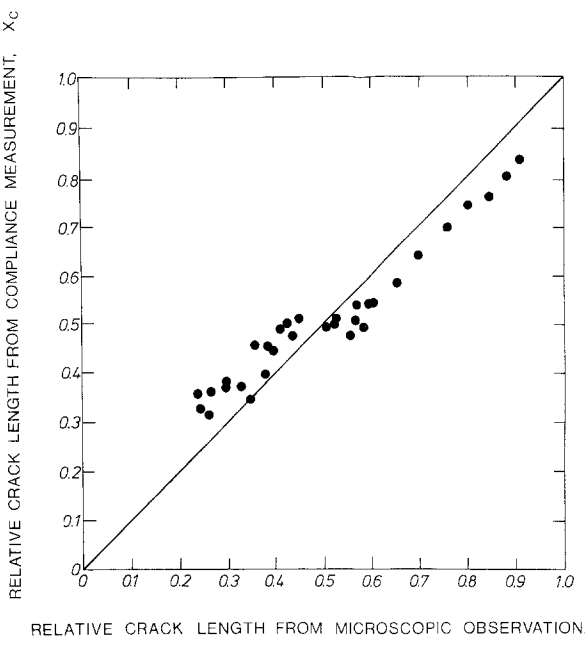

Figure 2 Comparison of relative crack length data determined microscopically and from compliance measurement.

the expression

$$d\lambda/dX = C_1 Y^2 X \tag{4}$$

is obtained which relates the derivative of the specimen compliance to the K-calibration factor Y. E' is the reduced Young's modulus of the material for plane strain conditions ($E' = E/(1-\nu^2)$, where ν is Poisson's ratio). C_1 is a constant depending on the test and specimen geometry. Integrating Equation 4 and inserting the compliance of the unnotched specimen for the integration constant yields in the case of pure bending

$$\lambda(X) = [9(l-e)^2/2bh^2E'] \left[\int_0^X Y^2(X')X' \, dX' + (l+2e)/18h \right], \tag{5}$$

with l and e the major and the minor span respectively.

Equation 5 may be used to evaluate crack length values from measured compliance data. In contrast to the result of double torsion specimens [11], Equation 5 cannot be solved for X as a function of λ. However, the right side of the equation can be computed by steps for any given X value using K-calibration factors reported in the literature. For $0.15 \leqslant X \leqslant 0.60$, the polynomial given by Gross and Srawley [14] was used, and for $0.50 \leqslant X \leqslant 0.80$ an analytical expression published by Wilson [15] was taken. Wilson's formula has been verified experimentally in this laboratory up to $X = 0.91$ [12].

The accuracy of the experimental results was checked on a set of precracked specimens. The vertical sidefaces of the specimens had been polished, and the relative crack length was determined under the microscope (X_M) and from the compliance (X_C). In Fig. 2, X_C is plotted against X_M. At large crack length values, $X > 0.5$, the agreement between X_M and X_C is satisfactory and lies within the estimated error limits of about 6%. The slope is given correctly as compared to the 45° straight line. At smaller crack length, $X < 0.5$, the deviation of the data points from the straight line is substantial in some cases. This is due to the weak dependence of the specimen compliance on the crack length in this region. Another reason for the limited accuracy of the method might be the bowing of the crack front. Nevertheless, the determination of the compliance crack length X_C is thought to be sufficiently exact.

The total crack length c in a specimen which has been loaded beyond its elastic limit is given by the sum of the initial notch depth c_0 and the length of the sub-critical crack extension Δc:

$$c = c_0 + \Delta c. \tag{6}$$

The notch depth was determined microscopically. The total crack length was obtained in the following way: Immediately after the crack extension loading a second experiment was carried out where the load remained within the elastic region of the

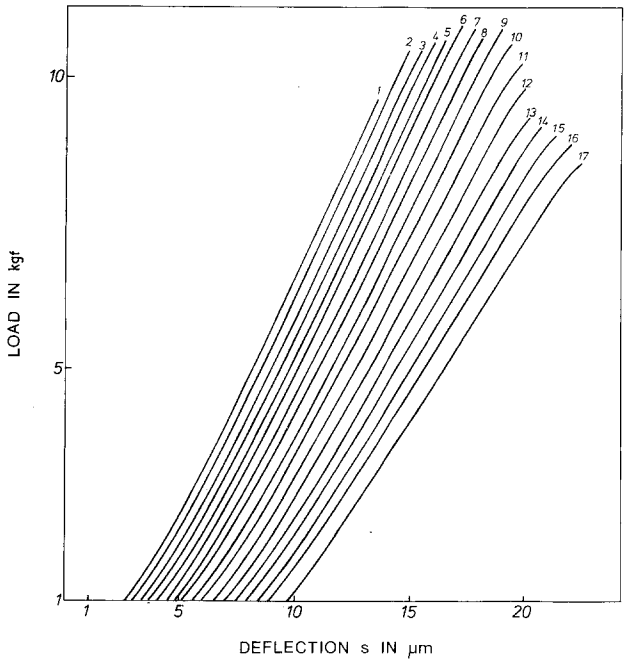

Figure 3 Load–deflection record of repeated loading of a notched bend specimen beyond the elastic region.

specimen. From the load–deflection record of the second experiment the specimen compliance was determined and hence the total crack length achieved during the former experiment was computed in the way described above.

3.2. Dependence of crack length on stress intensity factors

The deviation of the load–deflection curve at a load $P > P_0$ to larger deflections is caused by subcritical crack extension. This can be demonstrated

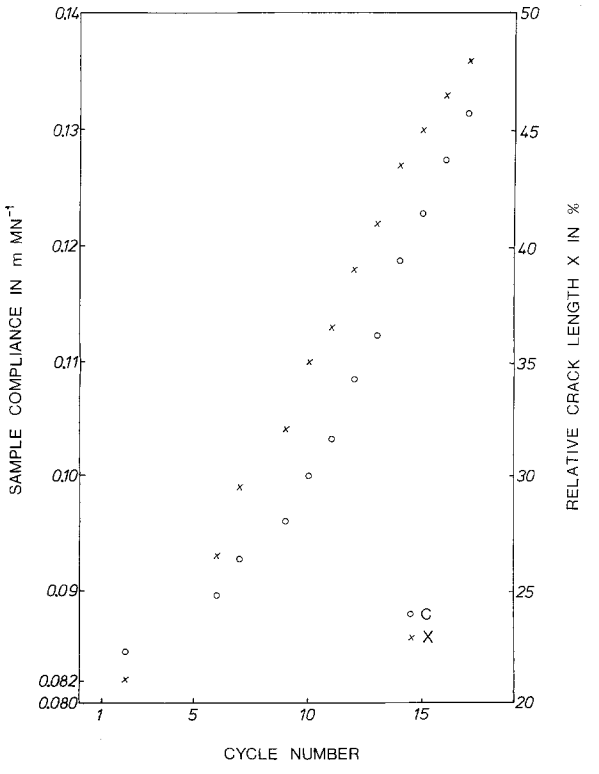

Figure 4 Sample compliance and relative crack length versus number of loading cycles in Fig. 3.

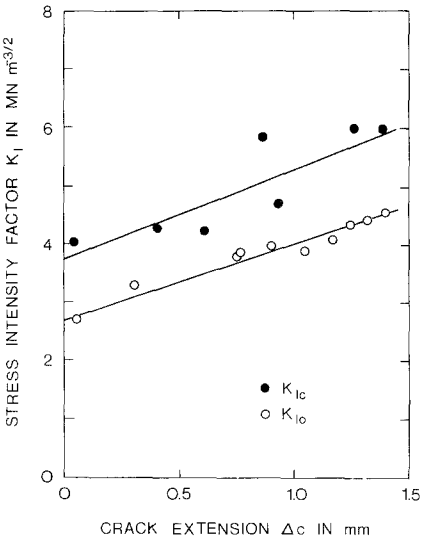

Figure 5 Dependence of K_{I_0} and K_{IC} on the crack extension Δc.

by repeated cycles of loading beyond the elastic limit and unloading. Fig. 3 shows a load–deflection record of a sample which has been loaded 17 times. For better resolution, the origins of the single plots are shifted to the right. Each curve shows a "yield point" P_0 when the crack starts to move again, the slope of the following curve being smaller. The specimen compliance which results from each slope versus the number of loading cycles is plotted in Fig. 4. The data were corrected for the machine deformations before plotting. The crack length as determined from the compliance is also plotted in Fig. 4. An average relative crack length increase ΔX of about 0.02 is achieved during one loading cycle, corresponding to an absolute crack extension $\Delta c \approx 0.1$ mm. Adding all single propagation steps the crack elongates through a distance of 1.4 mm.

From the load value P_0 and the actual crack length c, a stress intensity factor K_{I0} may be obtained at the onset of crack propagation. It is plotted in Fig. 5 as a function of the actual distance from the notch root $\Delta c = c - c_0$ (open circles). Looking at Fig. 5 it is surprising that the stress intensity factor to restart the crack, K_{I0}, depends on the natural crack length in the material. It increases by about 70% from 2.7 to 4.6 MN m$^{-3/2}$.

Once this effect had been known an attempt was made to find out whether even the critical stress intensity factor K_{IC} may be influenced by the length of a pre-existing natural crack. A series of samples was notched to about 25% of the specimen width and then slowly broken to different crack lengths Δc in controlled fracture experiments. The samples contained an atomically sharp crack which is an essential requirement in fracture mechanics testing at least of ductile materials, but which is not necessarily to be met when brittle materials are tested. This has been shown to be valid in polycrystalline alumina by Bertolotti [16]. The pre-cracked samples were loaded using a high cross-head speed and a small lower span for catastrophic failure to occur. The K_{IC} values obtained at different total crack lengths $c = c_0 + \Delta c$ are plotted in Fig. 5 as a function of the natural crack length Δc (closed circles). K_{IC} also exhibits an increasing trend with Δc which is nearly parallel to the rise of K_{I0}. The starting value at zero natural crack length is about 3.8 MN m$^{-3/2}$ and agrees with data reported in the literature, e.g. Swanson [17], and by Simpson [18].

The observed dependence of K_{IC} on crack length is contradictory to the predictions of fracture mechanics and to other experimental studies, for example to the work of Davidge and Tappin [19] who have not found any crack length effect on the critical energy for fracture initiation γ_I which is directly related to K_{IC} through the Irwin equation [13] $K_{IC}^2 = 2\gamma_I E'$. However, these investigations have been performed on samples containing not natural cracks, but sawn notches. In a further paper, Davidge and Tappin [20] report investigations to study the influence of different notch geometries on the critical fracture energy γ_I of alumina specimens. One batch of samples has been notched to a fixed depth before testing and the other batch has been notched and precracked to the same total depth as the solely machined specimens. For a natural crack length of $\Delta c =$ 0.5 mm, however, in this study, no effect of precracking on γ_I has been observed [20].

In contrast to these results our further investigations do in fact show a dependence of K_{IC} on Δc. A similar procedure was applied to the samples which had been tested to obtain the K_{IC} values of Fig. 5. The broken halves were prepared for repeated K_{IC} tests by notching each one to a depth which was equal to the total crack length c of the preceding experiment. The results of these K_{IC} measurements are shown in Fig. 6. The critical stress intensity factor remains constant when the notch depth is increased from 25 to 55% of specimen width, in contrast to the K_{IC} increase in the pre-cracked specimens which is also plotted

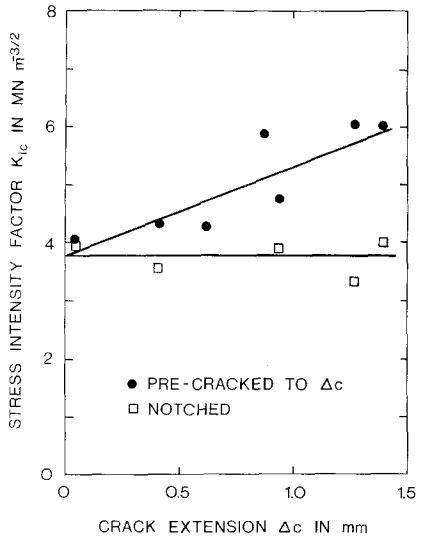

Figure 6 Critical stress intensity factor K_{IC} of pre-cracked and of solely notched specimens.

in Fig. 6 for comparison. This behaviour obviously has to be interpreted in terms of material properties instead of a geometrical size dependence.

4. Crack resistance curve

According to the R-concept of fracture mechanics [21, 22], the crack extension in a test piece subjected to increasing values of the energy release rate $\mathcal{G}_I$ (or stress intensity factor K_I) is governed by the crack extension resistance R of the material in question. As proposed by Krafft *et al.* [23], the crack extension resistance is an increasing function of the achieved crack length $\Delta c = c - c_0$. It describes the characteristic of the material to undergo a hardening process when a crack is extended, thus offering increasing resistance against further crack propagation. Whereas the existence of a bent R-curve is a well-known fact in plane-stress testing of thin ductile materials [24], similar results have been found recently for brittle high-strength metals under plane strain conditions by Munz [25].

The dependence of stress intensity factors to start the propagation of natural cracks, K_{I0}, and to obtain uncontrolled fracture, K_{IC}, respectively on the crack length as described in the previous section suggests that even a brittle material like alumina may show a bent crack resistance curve. Therefore, further experiments have been carried out to determine stress intensity factor values which must be applied to achieve a given crack length.

4.1. Single loading experiments

Controlled fracture experiments have been performed on notched specimens. The specimens were loaded to different deflections $s > s_0$ corresponding to load values P_i which lay between P_0 and the maximum load, and beyond the maximum load, and then unloaded. The achieved crack length c_i was determined from the load–deflection slope of a following experiment as well as from microscopic observation. Taking P_i and c_i, the stress intensity factor K_I to propagate a crack the distance Δc from c_0 to c_i was evaluated. It is shown in Fig. 7 as a function of the crack extension Δc. Considerable increase in K_I with Δc was again obtained.

4.2. Continuous evaluation of controlled fracture tests

In a controlled fracture test a slow and stable crack extension occurs through the test piece [10]. A balance is maintained during crack growth between the released energy $\mathcal{G}_I$ and the consumed energy to create the fracture surface, R. Following a proposal made by Kleinlein [26], a stress intensity value can be attributed to each point of

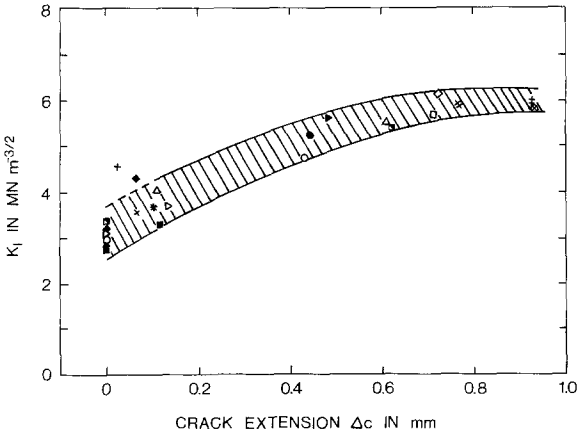

Figure 7 Stress intensity factor K_I at the point of unloading as a function of the achieved crack extension Δc.

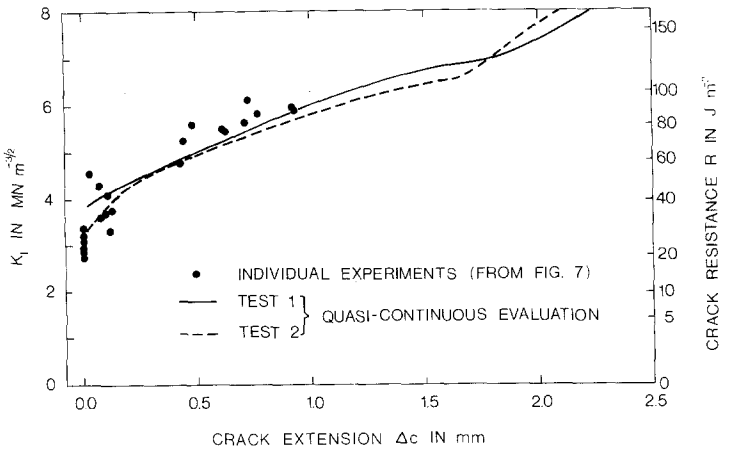

Figure 8 Quasi-continuous evaluation of controlled fracture tests. The data points of Fig. 7 are shown for comparison.

the load–deflection record of a controlled fractured brittle specimen. The crack length which pertains to a given load P_i can be determined from the instantaneous specimen compliance by drawing a straight line from P_i to the origin of the load–deflection plot and applying Equation 5. The deflection axis must have been corrected for the elastic deformations of the testing system. The load–deformation response of the bending apparatus can be recorded when a specimen is loaded with the lower rollers lying exactly below the upper rollers [26]. Thus, each set of load and deflection values on a continuous load–deflection record delivers, with the aid of a computer program, the stress intensity factor, the energy release rate, the crack length, and the crack extension Δc. Since the values of load and deflection can be taken from the record at any desired small distance, the conversion procedure is quasi-continuous.

The results of two converted records of controlled fracture experiments are given in Fig. 8, which shows a steady rise of K_I with respect to the crack extension. The evaluation is performed until a crack length of approximately 95% of the specimen width is reached. The data points of the single loading experiments of Fig. 7 are drawn in Fig. 8 for comparison. The astonishing fact in Fig. 8 is that the stress intensity factor K_I to drive a crack through the sample has to be increased by a factor of 2 when it is slowly moved from about 50% of the sample width to the upper face of the bend specimen. The required K_I values considerably exceed even the critical stress intensity factor K_{IC} of notched specimens.

5. Discussion

A consideration of the experimental results reveals the following: the values of K_{I0} ($\approx 2.7\,MN\,m^{-3/2}$) and K_{IC} ($\approx 3.8\,MN\,m^{-3/2}$) of the alumina material studied in the present work are independent of the notch depth c_0. A natrual crack of any desired length c which exceeds the notch depth by the amount $\Delta c = c - c_0$ may be introduced by stable crack propagation using the controlled fracture technique. The stress intensity factor to achieve Δc increases considerably with increasing natural crack length (Figs. 7 and 8). As Δc increases, K_{I0} and K_{IC} also increase (Fig. 5).

During slow and stable crack growth for every stage of propagation, an energy balance is maintained between the externally applied energy release rate $\mathcal{G}_I$ and the crack resistance R of the material. Therefore, the various stress intensity factors to start a crack from a given Δc (K_{I0} in Fig. 5), to drive a crack up to a given Δc (K_I in Fig. 7), and to move a crack continuously through the ligament (K_I in Fig. 8) virtually have the same physical meaning: as long as the crack moves slowly and in a controlled manner $\mathcal{G}_I$ is equal to R. The rise of the stress intensity factor when converted to R by use of the Irwin equation [13] gives the crack extension resistance of the material as a function of the crack length. The resistance against crack extension can be regarded as the "differential work of fracture", i.e. the energy consumption to create a small increment of fracture surface.

In terms of the R-curve concept of fracture mechanics the K_I increase in alumina shows a formal analogy to the crack resistance of metallic materials where the existence and bending of the R-curve is attributed to the development of the plastic zone ahead of the crack tip [24]. However, in the case of aluminium oxide plastic deformation processes during fracture can be certainly excluded, at least at room temperature [3].

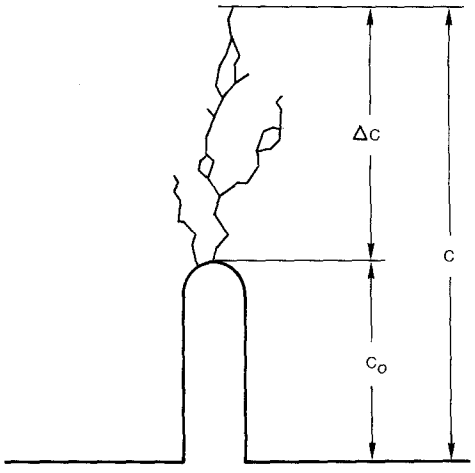

Figure 9 Schematic drawing of crack branching and joining in polycrystalline alumina.

When slow fracture occurs in alumina the material is separated along its grain boundaries. Thereby the crack may branch and multiple cracks may develop as depicted in Fig. 9. As a consequence the stress in the vicinity of the leading crack is released to some extent. When the crack surrounds some grains excess energy must be supplied to create the additional fracture surface. Since the crack front does not represent a straight line but has a three-dimensional angular appearance, mode II and III loading may occur and an interference between the fracture surfaces is expected to lead to additional energy consumption due to friction. For these reasons one can expect a branching crack which moreover generates a rough fracture surface to need an increased stress intensity factor and to consume enhanced fracture energy for its movement. The ratio of the work of fracture γ_F to the energy for fracture initiation γ_I, which is found to be about 3 to 4 in the present work and in the literature [19] can be understood on these assumptions as well as the observed increase in the stress intensity factors.

There are two experimental observations which confirm the proposed explanations:

(1) A weight loss of the bend specimens was determined after the controlled fracture test. It amounts up to about 10^{-3} g (corresponding to 10^5 grains of 20 μm grain size) and must be due to crack branching and converging;

(2) The branching and joining of cracks could be detected microscopically on polished side faces

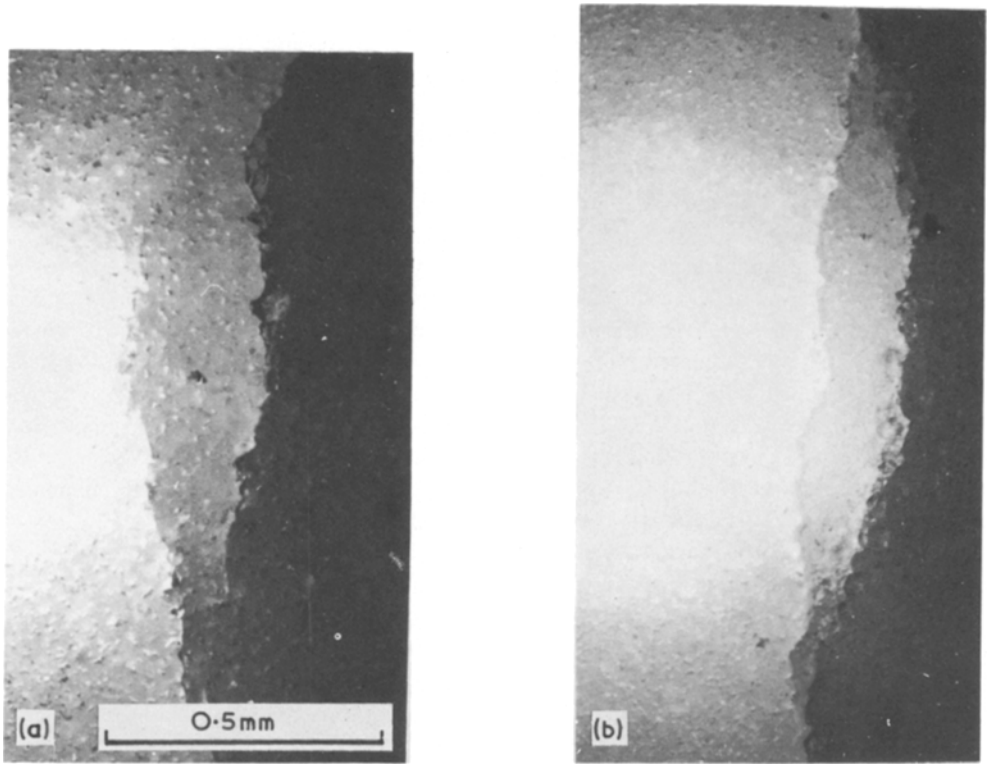

Figure 10 Experimental evidence for crack branching and rejoining. (a) A branch is left behind the main crack, (b) both branches rejoin. Crack propagation direction is from bottom to top.

of partially fractured bend specimens. Fig. 10 shows two examples.

From the experimental results the conclusion can be drawn that alumina becomes tougher with increasing natural crack length. This behaviour is expected to affect the properties of the material when loaded under mechanical or thermal shock conditions, because the shock strength of a ceramic material is mostly determined by its crack extension resistance.

Acknowledgements

This work was sponsored by Deutsche Forschungsgemeinschaft, DFG. The authors acknowledge the critical and helpful review of the manuscript by Professor B. Ilschner. Thanks are due to G. Wehner and R.B. Clegg for experimental assistance.

References

1. S. M. WIEDERHORN, Subcritical crack growth in ceramics, in "Fracture Mechanics of Ceramics", Vol. 2, edited by R.C. Bradt, D.P.H. Hasselman and F.F. Lange (Plenum Press, New York, 1974) pp. 613–46.
2. A. G. EVANS, *J. Mater. Sci.* 7 (1972) 1137.
3. S. M. WIEDERHORN, B. J. HOCKEY and D. E. ROBERTS, *Phil. Mag.* 28 (1973) 783.
4. R. W. DAVIDGE, J. R. McLAREN and G. TAPPIN, *J. Mater. Sci.* 8 (1973) 1699.
5. A. G. EVANS, *Int. J. Fracture* **10** (1974) 251.
6. A. G. EVANS and S. M. WIEDERHORN, *ibid* **10** (1974) 379.
7. S. N. ZHURKOV, *Int. J. Fracture Mech.* 1 (1965) 311.
8. R. STEVENS and R. DUTTON, *Mater. Sci. Eng.* 8 (1971) 220.
9. B. R. LAWN, *J. Mater. Sci.* **10** (1975) 469.
10. J. NAKAYAMA, *J. Amer. Ceram. Soc.* **48** (1965) 583.
11. K. R. McKINNEY and H. L. SMITH, *ibid* **56** (1973) 30.
12. H. HÜBNER and H. SCHUHBAUER, *Int. J. Fract.*, in press.
13. G. R. IRWIN, Fracture, in "Handbuch der Physik", Vol. 6, edited by S. Flügge (Springer Verlag, Berlin, 1958) pp. 551–90.
14. B. GROSS and J. E. SRAWLEY, NASA TN D-2603 (1965).
15. W. K. WILSON, *Eng. Fract. Mech.* **2** (1970) 169.
16. R. L. BERTOLOTTI, *J. Amer. Ceram. Soc.* **56** (1973) 107.
17. G. D. SWANSON, *ibid* **55** (1972) 48.
18. L. A. SIMPSON, *ibid* **56** (1973) 7.
19. R. W. DAVIDGE and G. TAPPIN, *J. Mater. Sci.* 3 (1968) 165.
20. *Idem, Proc. Brit. Ceram. Soc.* **15** (1970) 47.
21. J. E. SRAWLEY and W. F. BROWN, ASTM STP 381 (1964).
22. D. BROEK, "Elementary Engineering Fracture Mechanics" (Noordhoff, Leyden, 1974).
23. J. M. KRAFFT, A. M. SULLIVAN and R. W. BOYLE, Effect of dimensions on fast fracture instability of notched sheets, Proceedings of the Crack Propagation Symposium, Cranfield, England (1961) Vol. 1, pp. 8–28.
24. ASTM STP 527 (1973).
25. D. MUNZ, *Fortschr.-Ber. VDI-Z., Series 5* **20** (1975) 12.
26. W. KLEINLEIN, unpublished work.

Received 26 April 1976 and accepted 25 May 1976.